



# Ultrasound-targeted semaglutide-loaded PEG-nanoliposomes microbubble destruction protects diabetic cardiomyopathy by activating PI3K/Akt/Nrf2 signaling pathway

Jiawei Zhu<sup>a</sup>, Huiyang Wang<sup>b</sup>, Chunyang Yan<sup>a</sup>, Bin Li<sup>a</sup>, Bin Chen<sup>c,\*</sup>

<sup>a</sup> Department of Ultrasound, Ningbo Zhenhai People's Hospital, Ningbo 315202, Zhejiang province, PR China

<sup>b</sup> Department of Ultrasound Medicine, The First Affiliated Hospital, School of Medicine, Zhejiang University, Hangzhou 310003, Zhejiang province, PR China

<sup>c</sup> Department of Nephrology, Ningbo Zhenhai People's Hospital, Ningbo 315202, Zhejiang province, PR China

## ARTICLE INFO

### Keywords:

Semaglutide  
PEG  
Nanoliposome  
UTMD  
Diabetic cardiomyopathy  
PI3K/Akt/Nrf2 signaling pathway

## ABSTRACT

**Objective:** To investigate the ameliorative effect of Semaglutide-loaded PEG-nanoliposomes (Sem-PEG-lips) combined with ultrasound-targeted microbubble destruction (UTMD) on streptozotocin (STZ)-induced diabetic cardiomyopathy (DCM) in rodents and its potential mechanisms.

**Methods:** Sem-PEG-lips were prepared by the reverse phase evaporation method. Fifty STZ-induced diabetic rats were randomly divided into DCM model group, Sem or Sem-PEG-lips alone treatment group, UTMD + Sem group and UTMD + Sem-PEG-lips group (n = 10), respectively, and used the healthy rats as normal control. During the 12-week intervention, the weight and blood glucose levels of all rats were recorded. Myocardial injury and fibrosis were observed by using H&E and Masson staining. The activity of antioxidant enzymes and the expression levels of oxidative stress-related signaling pathway markers in myocardial tissues were measured by ELISA and western blotting method, respectively.

**Results:** Compared with DCM rats, the body weight and blood glucose levels of those in the UTMD + Sem-PEG-lips group were significantly increased and decreased, respectively (both p < 0.05). The results of H&E and Masson staining showed that myocardial fibrosis and apoptosis were both significantly improved in combination group (both p < 0.001). Further results of ELISA and Western blot analysis showed that the activity of antioxidant enzymes in ones received combination therapy were significantly higher than that in DCM model group (all p < 0.001), and the expression of PI3K/Akt/Nrf2 signaling pathway related proteins were significantly up-regulated (all p < 0.001), and all these changes were reversed by the treatment of PI3K inhibitor.

**Conclusion:** UTMD combined Sem-PEG-lips can reduce the oxidative stress of myocardial tissue in DCM rats by activating PI3K/Akt/Nrf2 signaling pathway, thereby improving diabetic myocardial injury.

## 1. Introduction

In recent years, the incidence of diabetes mellitus has risen rapidly, which has become a worldwide epidemic disease [1]. It is

\* Corresponding author.

E-mail address: [nbchenbing@hotmail.com](mailto:nbchenbing@hotmail.com) (B. Chen).

<https://doi.org/10.1016/j.heliyon.2023.e19873>

Received 22 June 2023; Received in revised form 2 September 2023; Accepted 4 September 2023

Available online 7 September 2023

2405-8440/© 2023 Published by Elsevier Ltd.

This is an open access article under the CC BY-NC-ND license

(<http://creativecommons.org/licenses/by-nc-nd/4.0/>).

reported that the number of diabetic patients in the world has exceeded 500 million, including 140 million in China [2]. There are many kinds of diabetic complications, of which the more fatal is diabetes related cardiovascular diseases [3]. Diabetic cardiomyopathy (DCM), as a serious complication of diabetes, can cause a series of abnormalities of myocardial structure and function, and eventually develop into heart failure, arrhythmia and cardiogenic shock [4]. In diabetic patients, it is easy to observe a variety of cardiac structural remodeling, such as ventricular dilation, significant interstitial fibrosis, cardiac diastolic and systolic dysfunction and left ventricular hypertrophy [3,5]. The pathogenesis of DCM is complex, and the specific mechanism has not been clearly studied [5]. As a basic clinical condition of diabetes, hyperglycemia can induce damage to multiple systems and organs, and also mediate oxidative stress, apoptosis and myocardial fibrosis, which are also important risk factors for DCM [6]. Diabetic patients are usually accompanied by hyperlipidemia, which can also increase the risk of cardiovascular disease [7]. According to the reported clinical statistics, about 67% of diabetic patients may die of serious cardiovascular diseases [8]. Therefore, it is of great clinical significance to actively study the prevention and treatment of diabetic cardiomyopathy.

Glucagon like peptide-1 (GLP-1) is an incretin that can be regulated by  $\beta$ -cell proliferation, regeneration and apoptosis to enhance insulin secretion and inhibit glucagon [9]. In addition, GLP-1 has been shown to ameliorate myocardial injury by reducing glycated hemoglobin and body weight and reducing inflammatory responses in patients [10]. Semaglutide (Sem), as a long-acting analog with high homology with GLP-1, has strong affinity with GLP-1 receptor (GLP-1R) *in vitro* [11]. Studies have shown that Sem shows good effectiveness and safety in glycemic control and long-term prognosis of cardiovascular disease in diabetic patients [12]. In addition, several clinical studies have shown that Sem can effectively increase the survival rate of patients after myocardial infarction and improve the cardiac functions of diabetic patients [13]. A meta-analysis showed that Sem could reduce the risk of cardiovascular death in patients with diabetes by 12%, the risk of nonfatal stroke by 16%, and the risk of heart failure by 9% [14]. Therefore, the application of SEM in the treatment of diabetic cardiomyopathy is supported by its clinical evidence.

Nanoliposomes are an effective drug delivery carrier with particle size of 10–1000 nm, which can penetrate the complete capillary and endothelial space, and can be taken up by most cells [15]. In addition, nanoliposomes also have the advantages of high drug loading, slow drug release, high stability, and reduced drug dosage [15]. Previous studies have confirmed that compared with traditional nanoliposomes, pegylated long circulating nanoliposomes loaded with drugs can prevent the drug loaded nanocarriers from being phagocytosed and degraded by the body's autoimmune system, such as phagocytes, and prolong their circulation time in the body, thus giving better play to the slow-release or controlled-release characteristics [16]. However, other strategies to increase selectivity for cardiac tissue are still needed and will improve the delivery of drugs to the heart without causing unnecessary harm to other tissues of the body.

Ultrasound-targeted microbubble destruction (UTMD) is a useful tool to promote drug specific delivery to certain organs [17]. Data from several preclinical studies have shown that UTMD technology can be effective in improving the selective release of drugs from liposomes in animal organs [18]. After intravenous injection, microbubbles can reach the myocardial tissue and be destroyed by ultrasound beam, and the resulting cavitation effect can enhance the release of drugs from liposomes at the ultrasound site [18]. UTMD-mediated nanocarrier delivery systems have low toxicity and low immunogenicity compared to other gene or drug delivery modalities. In addition, the Nano delivery system is non-invasive and highly reproducible by intravascular injection into the body. Most importantly, UTMD technology can enhance the targeting of nanocarriers and increase the transfection rate, and drugs or genes can be selectively delivered to designated regions of interest, thereby reducing the toxicity of systemic administration and reducing systemic reactions. Therefore, UTMD technology is expected to be an effective strategy to achieve targeted delivery of SEMs to myocardial tissue.

In this study, SEM was encapsulated in PEGylated nanoliposomes as a long circulating, and then combined with UTMD in DCM rat model to improve the myocardial injury induced by STZ in diabetes and its potential mechanism.

## 2. Materials and methods

### 2.1. Materials

Streptozotocin (STZ), poloxamer 188, gelatin and LY294002 were purchased from Sigma Aldrich (St Louis, Mo, USA); Semaglutide (purity 99%) was purchased from Shanghai Kaishi Biotechnology Co., Ltd (Shanghai, China); H&E staining kit and Masson trichrome staining kit were purchased from Solarbio Biotechnology Co., Ltd (Beijing, China); Collagen I, Collagen III, TGF- $\beta$ 1 and the ELISA kits for Malondialdehyde (MDA), Superoxide Dismutase (SOD), Glutathione Peroxidase (GSH-Px) and Catalase (CAT) were purchased from Sigma Aldrich (St Louis, Mo, USA); Rabbit anti-mouse PI3K, Akt, p-Akt, Nrf2, SOD2, NQO1, and  $\beta$ -Actin primary antibody and Goat anti-rabbit IgG secondary antibody were purchased from Abcam (Cambridge, UK). One touch ultra blood glucose meter and blood glucose test paper were purchased from Johnson and Johnson, Ltd (New Jersey, USA).

### 2.2. Preparation and characterization of Sem-PEG-lips

The PEGylated nanoliposomes loaded with Sem were prepared by reverse phase evaporation method [19]. The Sem lyophilized powder was dissolved in 20% poloxamer 188. The Sem solution with a concentration of 10 mg/mL was prepared. Subsequently, it was mixed with 2% gelatin aqueous solution at a ratio of 1:2 and rapidly dispersed by ultrasound (100 W, 15 s). After freeze-drying, Sem lyophilized powder was obtained. The above Sem lyophilized powder was dispersed in 4 mL *tert*-butyl alcohol containing DSPE-PEG2000 (PEGylated phospholipid) and cholesterol, and ultrasonic dispersion was performed for 20 s (100 W) at room temperature. After freeze-drying, drug loaded PEGylated nanoliposomes (Sem-PEG-lips) were obtained. SEM was isolated from the

Sem-PEG-lips suspension by ultracentrifugation. The concentration of Sem in the centrifugal supernatant was determined by HPLC. Encapsulation efficiency (%) = (total supernatant Sem)/total Sem  $\times$  100%.

### 2.3. Animals

SPF grade male Sprague Dawley (SD) rats (8–10 weeks old, weight 200–250 g) were purchased from Hangzhou Medical College (Hangzhou, Zhejiang). The feeding environment was strictly controlled with standard ventilation of constant temperature ( $25 \pm 1^\circ\text{C}$ ) and 50% constant humidity, and the light was alternated regularly for 12 h every day. After one week of adaptive feeding, rats were randomly selected to receive a single intraperitoneal injection of 1% Streptozotocin (STZ) at the dose of 70 mg/kg [20]. The blood glucose level was measured through the tail vein on the day 1, 3, 7 after injection by using glucose meter and blood glucose test paper. The type I diabetic rats with stable blood glucose level above 16.7 mmol/L and polydipsia, polydipsia and polyuria were selected. Then diabetic rats were randomly divided into DCM model group, Sem alone treatment group, Sem-PEG-lips alone treatment group, UTMD + Sem group and UTMD + Sem-PEG-lips group, with 10 rats in each group. After completing the first round of experiments, diabetic rats were prepared according to the above modeling and divided into DCM model group, UTMD + Sem-PEG-lips group, and UTMD + Sem-PEG-lips + LY294002 group for rescue experiments. In addition, normal rats were used as the normal control group, and equal doses of citric acid buffer were injected intraperitoneally, and they were raised under the same conditions.

Rats in each group were anesthetized by intraperitoneal injection of 3% sodium pentobarbital, and rats in normal control group and DCM group were injected with 1 mL normal saline via tail vein. The Sem group was injected with 10  $\mu\text{g}/\text{kg}$  of Sem solution; The Sem-PEG-lips group was injected with 10  $\mu\text{g}/\text{kg}$  of Sem-PEG-lips solution; The UTMD + Sem group was injected with 10  $\mu\text{g}/\text{kg}$  Sem solution; In the UTMD + Sem-PEG-lips group, 10  $\mu\text{g}/\text{kg}$  Sem-PEG-lips solution. In the UTMD + Sem-PEG-lips + LY294002 group, 10  $\mu\text{g}/\text{kg}$  Sem-PEG-lips solution and 10  $\mu\text{g}/\text{kg}$  LY294002 solution dissolved in dimethyl sulfoxide. Rats were shaved in the precordial area and fixed in the supine position. The ultrasonic linear array probe was placed in the precordial region of rats, and the coupling agent was filled between the probe and the skin. The short axis view of the left ventricle at the level of papillary muscle was taken, and the focus depth was 3.5–4.0 cm. When the ultrasonic diagnostic instrument receives the signal of microbubbles entering the heart cavity, it uses the microbubble explosion function of the machine to repeatedly break the microbubbles (mechanical index = 1.9, ultrasonic duration 10 s, repeat 3 times, interval 1 s, ultrasonic frequency 14 MHz), producing UTMD effect until the microbubbles completely disappear. Rats in each group received corresponding intervention for 12 weeks, three times a week. The body weight and blood glucose of all rats were measured before and after drug intervention. After 12 weeks of intervention, all rats received ultrasonic cardiac function detection, and the left ventricular end diastolic diameter (LVEDd), left ventricular end systolic diameter (LVESD), left ventricular end diastolic volume (LVEDV), left ventricular end systolic volume (LVESV), left ventricular ejection fraction (LVEF) and left ventricular short axis shortening (LVFS) were measured.

### 2.4. ELISA and histopathology analysis

After treatment, all rats were euthanized. The heart was removed, and the myocardial tissue was cut at the level of the papillary muscle of the left ventricle, and paraffin sections were prepared. The remaining myocardial tissue was frozen in liquid nitrogen for ELISA analysis and Western blot analysis. The paraffin sections of 5  $\mu\text{m}$  thickness were stained according to the instructions of H&E staining kit and Masson staining kit. Pathological changes in myocardial tissue were evaluated according to the H&E staining score as previously described [21]. Myocardial collagen volume fraction was analyzed using Image-Pro Plus 6.0 software. Light microscope was used for observation. Take part of frozen myocardial tissue and analyze collagen I, collagen III and TGF- $\beta$ 1 in myocardial tissue according to the instructions of commercial ELISA kits. In addition, MDA levels and the activities of SOD, GSH PX and CAT were also measured by commercial ELISA kits according to the instructions.

### 2.5. Western blot

The expression of PI3K, Akt, p-Akt, Nrf2, SOD2 and NQO1 in myocardial tissue was detected by Western blotting analysis. Take a small amount of frozen myocardial tissue block, cut it into pieces, and add 180  $\mu\text{L}$  Ripa lysate (containing 20  $\mu\text{L}$  PMSF) was mixed and placed on ice for 30 min. After lysis, the tissue homogenate was centrifuged at  $4^\circ\text{C}$  (12000g, 10min), and the supernatant was taken for Western blot analysis. Protein electrophoresis was performed by SDS-PAGE, and the proteins were subsequently transferred to PVDF membranes. Then the PVDF membranes were blocked with 5% skim milk for 2 h, and then added with primary antibodies of PI3K, Akt, p-Akt, Nrf2, SOD2, and NQO1 (1:1000), respectively, and incubated overnight at  $4^\circ\text{C}$ . The next day, the membrane was washed thoroughly by tbst, and the secondary antibody (1:10000) was added and incubated at room temperature for 1 h. The  $\beta$ -Actin was used as an internal reference for gray scale analysis using Image-pro 6.0. All band density was first normalized to the  $\beta$ -actin, and then normalized to the normal control group.

### 2.6. Statistical analysis

SPSS 27.0 was used for statistical analysis in current work. Data are expressed as mean  $\pm$  SD, and *t*-test was used for comparison between two groups. P value below 0.05 is considered as statistically significant.

### 3. Results

#### 3.1. Characterization of Sem-PEG-lips

The appearance and cryo EM observation results of Sem-PEG-lips are shown in Fig. 1A and B, respectively. The Sem encapsulated liposomes were uniformly distributed and generally spherical in shape with a diameter of nearly 100 nm. The average particle size of Sem-PEG-lips was  $108.9 \pm 1.3$  nm, PDI was 0.244, and zeta was  $-12.82$  mV, respectively, as determined by nano-laser particle size analyzer (Fig. 1C–D). Among them, the results of zeta potential suggest that the liposomes may be stable with minimal aggregation. The encapsulation efficiency of Sem-PEG-lips was determined to be  $89.1 \pm 1.5\%$ , indicating that semaglutide can be effectively encapsulated by liposomes.

#### 3.2. UTMD combined with Sem-PEG-lips improved diabetic symptoms and myocardial injury in DCM rats

Random and fasting blood glucose levels of diabetic rats were measured after continuous 12 weeks treatment. Results as shown in Fig. 2A–B, compared with normal rats, diabetic rats had significantly higher random blood glucose and fasting blood glucose levels at week 0 and week 12 (both  $p < 0.001$ ). After different modalities of Sem treatment, the random and fasting blood glucose levels of diabetic rats were all significantly reduced. It is worth noting that compared with Sem, Sem-PEG-lips can play a similar role in improving blood glucose, suggesting that the preparation of Sem into liposome drug form does not change its basic blood glucose control ability. In addition, the change trend of HbA1c was similar to that of blood glucose. The body weight changes of the rats in all group was measured before and after treatment, and that of the normal rats increased normally during the 12-week treatment. However, compared with normal rats, the weight of diabetic rats decreased significantly ( $p < 0.001$ ). Both chronic treatment of Sem and Sem-PEG-lips both significantly reversed the abnormal body weight changes of diabetic rats.

#### 3.3. UTMD combined with Sem-PEG-lips improved diabetic myocardial injury in DCM rats

The injury of myocardial tissues from the DCM rats was further evaluated by H&E staining after 12-week treatment. As shown in Fig. 3A–B the myocardial structure of normal rats is clear, the cardiomyocytes are closely arranged, and the myofibrils are not denatured and damaged. On the contrary, the myocardial tissues of diabetic rats showed vacuolization and necrosis around the nucleus, and myofibrillar degeneration was obvious. In addition, significant improvements in myocardial structural abnormalities were observed in the different forms of Sem treated groups. In particular, cardiomyocyte vacuolization and myofibril loss were not detected in the UTMD combined with Sem-PEG-lips group.

Subsequently, the serum indicators related to diabetic myocardial injury were detected. As shown in Fig. 3C–E, compared with

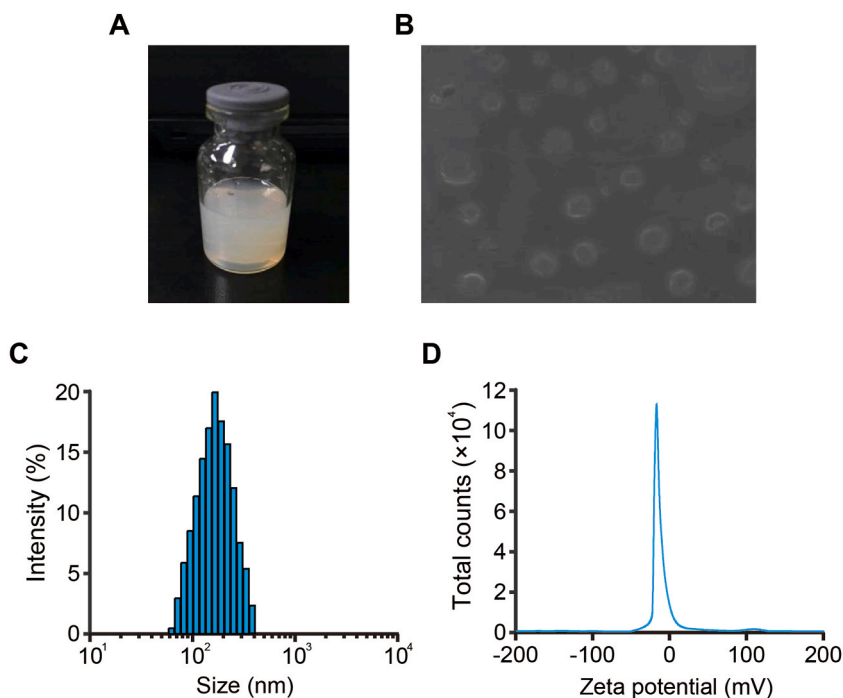


**Fig. 1.** Characterization of Sem-PEG-lips. (A) Visual observation, (B) scanning electron microscopy, (C) particle size distribution and (D) zeta potential of Sem-PEG-lips.

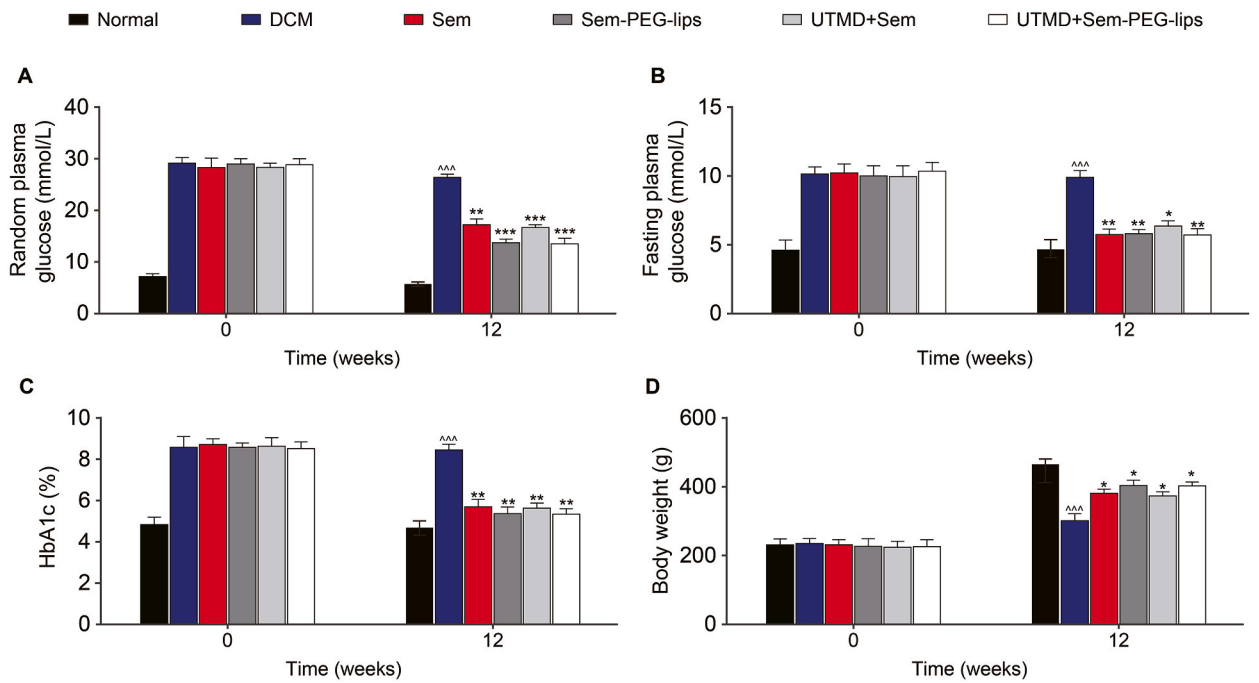


**Fig. 2.** Effects of UTMD combined Sem-PEG-lips on diabetic symptoms in DCM rats. (A) Random plasma glucose, (B) fasting plasma glucose, (C) HbA1c%, and (D) body weight of DCM rats after consecutive 12 weeks intervention. Data presented as Mean  $\pm$  SD,  $n = 10$ . \* $p < 0.05$ , \*\* $p < 0.01$ , \*\*\* $p < 0.001$  vs. DCM group.

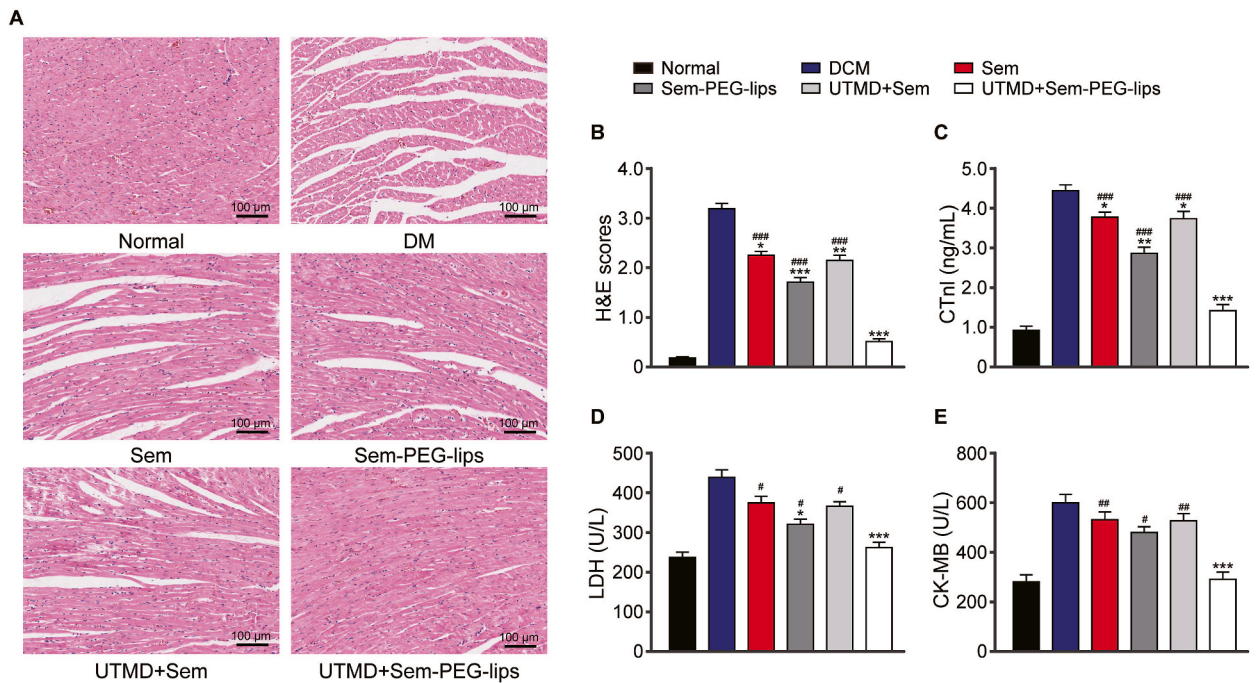


**Fig. 3.** Effects of UTMD combined Sem-PEG-lips on myocardial injury in DCM rats. (A) Representative images of H&E stain in myocardial tissue (Scale bars ( $\times 200$ ): 100  $\mu$ m), and serum levels of (B) CTnI, (C) LDH, and (D) CK-MB of DCM rats after consecutive 12 weeks intervention. Data presented as Mean  $\pm$  SD,  $n = 10$ . \* $p < 0.05$ , \*\* $p < 0.01$ , \*\*\* $p < 0.001$  vs. DCM group; # $p < 0.05$ , ## $p < 0.01$ , ### $p < 0.001$  vs. UTMD + Sem-PEG-lips group.

normal rats, the level of CTnI in the serum of DCM rats was significantly increased ( $p < 0.001$ ), and the activities of LDH and CK-MB were significantly increased (both  $p < 0.001$ ). In addition, different forms of Sem treatment could reverse these indicators of myocardial injury (both  $p < 0.05$ ). Consistent with the results of H&E staining, UTMD combined with Sem-PEG-lips could maximally reduce the level of CTnI and the activities of LDH and CK-MB (both  $p < 0.001$ ). It is worth noting that the activities of LDH and CK-MB in serum of UTMD combined with Sem-PEG-lips rats were not significantly different from those of normal rats ( $p > 0.05$ ). Above results showed that UTMD combined with Sem-PEG-lips could significantly improve myocardial injury in diabetic rats.

### 3.4. UTMD combined with Sem-PEG-lips improved cardiac function in DCM rats

After 12 weeks of continuous treatment, the cardiac function parameters of DM rats were observed by echocardiography. As shown in Fig. 4A–F, compared with normal rats, the LVEDd, LVESD, LVEDV and LVESV of DM rats were significantly increased (all  $p < 0.05$ ). In addition, the LVEF and LVFS were significantly decreased compared with the normal control group (all  $p < 0.05$ ), indicating that the DCM rat model was successfully established. After different forms of Sem intervention, the cardiac function parameters of DCM rats were significantly reversed (all  $p < 0.05$ ). In particular, the UTMD combined with Sem-PEG-lips group had the most significant improvement in cardiac dysfunction (all  $p < 0.01$ ). It is worth noting that the levels of LVEDd, LVESD, LVEDV, LVESD, LVEF and LVFS in the UTMD combined with Sem-PEG-lips group were not significantly different from those in the normal group (all  $p > 0.05$ ), which suggested that ultrasound targeted destruction of Sem-PEG-lips can significantly improve the cardiac function of DCM rats.

### 3.5. UTMD combined with Sem-PEG-lips improved myocardial fibrosis in DCM rats

The effect of Sem-PEG-lips combined with UTMD on myocardial fibrosis in DCM rats were assessed by Masson staining. As shown in Fig. 5A–B, the collagen deposition was stained blue, while red represented normal myocardial tissue. Compared with the normal group, the collagen content in the interstitial zone of cardiomyocytes in DCM group was significantly increased. In addition, the myocardial tissue of rats in different forms of Sem treatment groups showed different degrees of collagen deposition reduction. Subsequently, the levels of fibrosis marker proteins in myocardial tissue were analyzed by ELISA. As shown in Fig. 5C–E, the collagen I, collagen III, and TGF- $\beta$ 1 in myocardial tissue of DCM rats were all significantly increased (all  $p < 0.05$ ). While compared with the DM group, the protein levels of these fibrosis markers in myocardial tissue were significantly decreased in the different forms of Sem administration groups (all  $p < 0.05$ ), which had a similar trend with the results of the Masson staining. Among them, collagen I, collagen III and TGF- $\beta$ 1 in the myocardium of rats in the Sem-PEG-lips combined with UTMD group level was the lowest, followed by the Sem-PEG-lips group. Interestingly, there was no significant difference between the levels of fibrosis marker proteins in the myocardium of rats in the Sem-PEG-lips combined UTMD group and those in the normal group (all  $p > 0.05$ ), indicating that ultrasound targeted destruction of Sem-PEG-lips can significantly improve myocardial fibrosis in DCM rats.

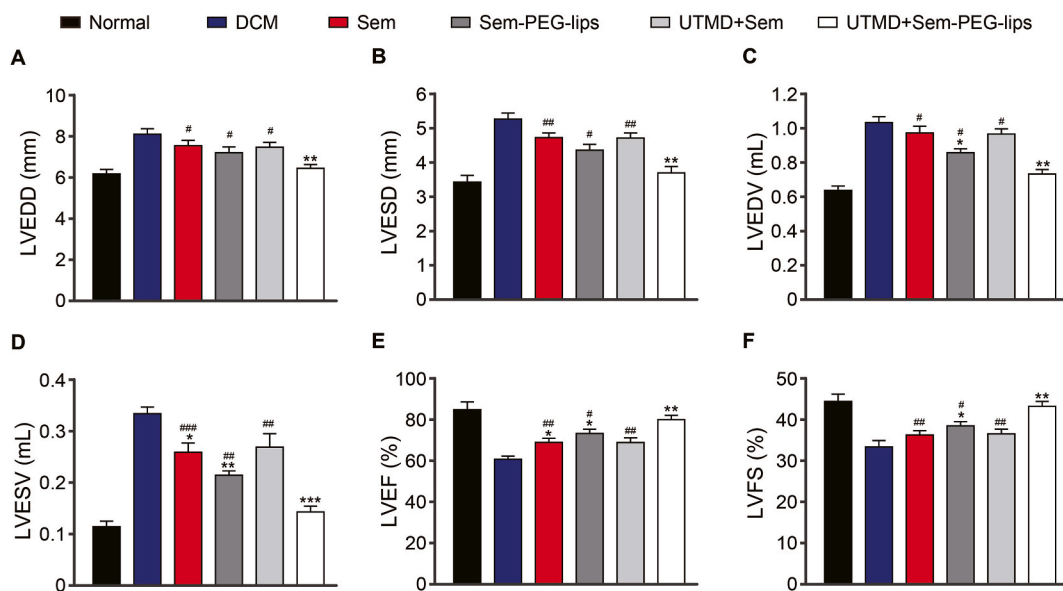


**Fig. 4.** Effects of UTMD combined Sem-PEG-lips on cardiac functions of the DCM rats. (A) LVEDD, (B) LVESD, (C) LVEDV, (D) LVESV, (E) LVEF and (F) LVFS in DCM rats after consecutive 12 weeks intervention. Data presented as Mean  $\pm$  SD, n = 10. \* $p < 0.05$ , \*\* $p < 0.01$ , \*\*\* $p < 0.001$  vs. DCM group; # $p < 0.05$ , ## $p < 0.01$ , ### $p < 0.001$  vs. UTMD + Sem-PEG-lips group.

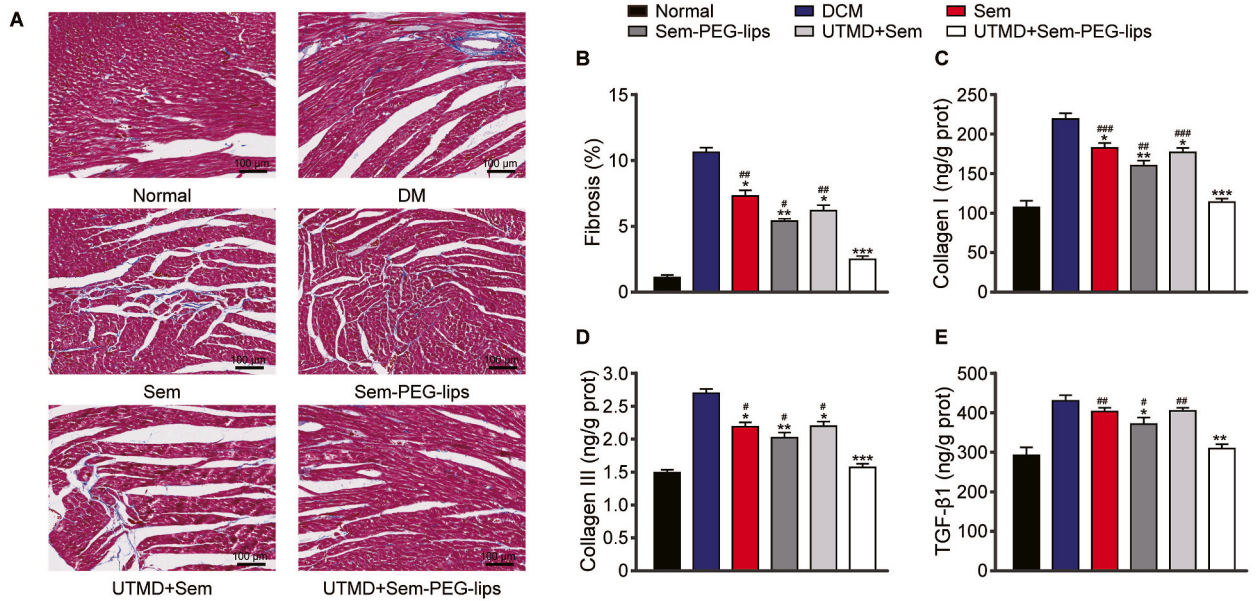


**Fig. 5.** Effects of UTMD combined Sem-PEG-lips on myocardial fibrosis in DCM rats. (A) Representative images of Masson stain (Scale bars (× 200): 100 μm) and the contents of (B) Collagen I, (C) Collagen III, and (D) TGF-β1 in myocardial tissue of DCM rats after consecutive 12 weeks intervention. Data presented as Mean ± SD, n = 10. \**p* < 0.05, \*\**p* < 0.01, \*\*\**p* < 0.001 vs. DCM group; #*p* < 0.05, ##*p* < 0.01, ###*p* < 0.001 vs. UTMD + Sem-PEG-lips group.

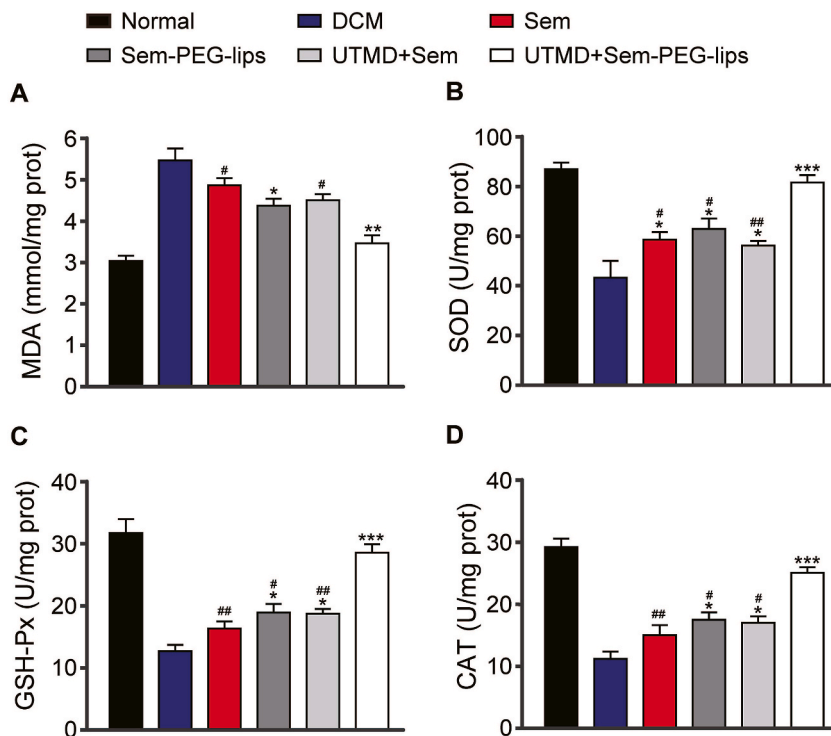


**Fig. 6.** Effects of UTMD combined Sem-PEG-lips on oxidative stress in DCM rats. Quantitative analysis of (A) MDA contents and the activities of (B) SOD, (C) GSH-Px, and (D) CAT in myocardial tissue of DCM rats after consecutive 12 weeks intervention. Data presented as Mean ± SD, n = 10. \**p* < 0.05, \*\**p* < 0.01, \*\*\**p* < 0.001 vs. DCM group; #*p* < 0.05, ##*p* < 0.01, ###*p* < 0.001 vs. UTMD + Sem-PEG-lips group.

3.6. UTMD combined with Sem-PEG-lips decreased the oxidative stress of myocardial tissues from DCM rats

To explore the effect of Sem-PEG-lips combined with UTMD on oxidative stress in the cardiac tissues of DCM rats, the MDA level and the activities of different antioxidant enzymes were analyzed by ELISA method. As shown in Fig. 6A–D, the level of MDA in myocardial tissue of DCM group was significantly higher than that of normal control group ( $p < 0.05$ ), while the activities of antioxidant enzymes including SOD, GSH PX and cat were significantly lower than that of normal control group, suggesting the occurrence of oxidative stress in DCM rats.

In addition, compared with DCM rats, the serum MDA levels of rats in different Sem treatment groups were all significantly decreased (all  $p < 0.01$ ), while antioxidant enzyme activities were significantly increased (all  $p < 0.05$ ). Among all Sem treatment groups, Sem-PEG-lips combined with UTMD had the best effect on improving the antioxidant capacity *in vivo*, indicating that ultrasound targeted destruction of Sem-PEG-lips can significantly improve the oxidative stress in DCM rats.

3.7. Effect of UTMD combined with Sem-PEG-lips on expression of PI3K/Akt/Nrf2 signaling pathway in myocardial tissue of DCM rats

Oxidative stress is one of the important causes of pathophysiological changes in diabetes. In order to explore the potential mechanism of Sem-PEG-lips combined with UTMD in improving oxidative stress in cardiac tissue of DCM rats, the expression of PI3K/Akt/Nrf2 signaling pathway was analyzed by Western blot. As shown in Fig. 7, compared with the normal control group, the expression level of PI3K and the phosphorylation level of Akt in the myocardial tissue of DCM group rats were significantly decreased (all  $p < 0.01$ ). After treatment with different forms of Sem, the expression of PI3K and the phosphorylation level of Akt increased to varying degrees (all  $p < 0.05$ ). In addition, the expression levels of PI3K and *p*-Akt in Sem-PEG-lips combined with UTMD group were significantly higher than those in other Sem treatment groups (all  $p < 0.05$ ). In addition, the expression levels of Nrf2, SOD2 and NQO1 in cardiac tissue of DCM rats were all significantly lower than those of normal rats (all  $p < 0.001$ ). It was also found that compared with untreated DCM rats, the expression levels of Nrf2, SOD2 and NQO1 were up-regulated in different forms of Sem treatment groups (all  $p < 0.05$ ). In particular, the protein expression levels of Nrf2, SOD2 and NQO1 were the highest in the Sem-PEG-lips combined with UTMD treatment group. The above results indicated that ultrasound targeted destruction of Sem-PEG-lips could improve oxidative stress in DCM rats by activating PI3K/Akt/Nrf2 signaling pathway.

3.8. Inhibition of PI3K/Akt axis reversed the beneficial effect of UTMD combined with Sem-PEG-lips on diabetic myocardial injury in DCM rats

In order to verify that UTMD combined with Sem-PEG-lips can improve diabetic myocardial injury by activating PI3K/Akt axis, the expression of PI3K was inhibited by LY294002, as a PI3K inhibitor. As shown in Fig. 8A–C, UTMD combined with Sem-PEG-lips significantly up-regulated the expression of PI3K and the phosphorylation level of Akt (all  $p < 0.001$ ), but these changes were significantly reversed by LY294002 (all  $p < 0.001$ ). In addition, compared with the UTMD + Sem-PEG-lips group, the H&E score of myocardial tissue and the degree of myocardial fibrosis in the UTMD + Sem-PEG-lips + LY294002 group were significantly increased (all  $p < 0.001$ , Fig. 8D–E). Moreover, the serum indexes related to myocardial injury, including CTnl, LDH and CK-MB, in LY294002

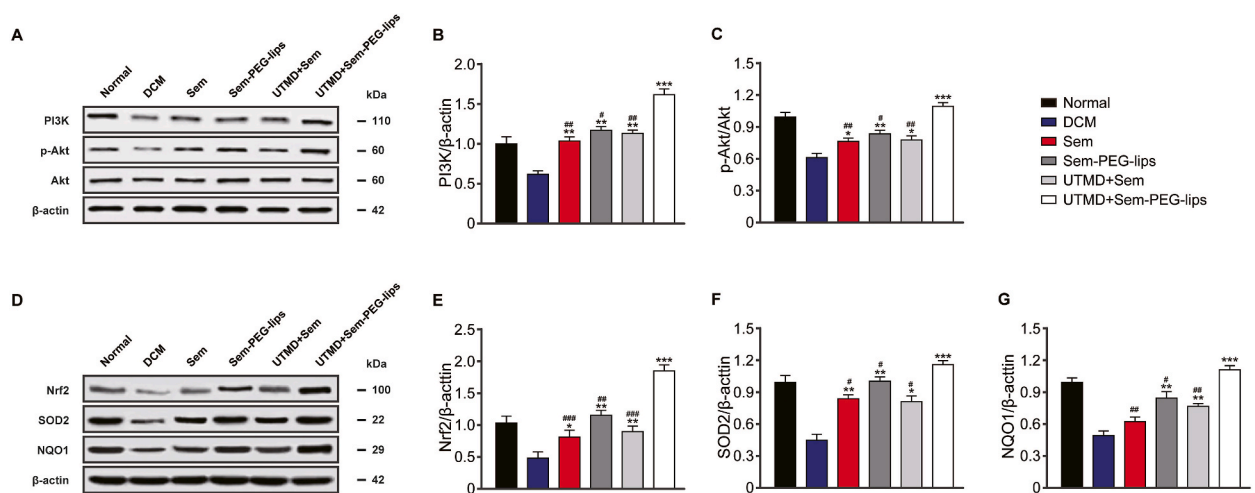
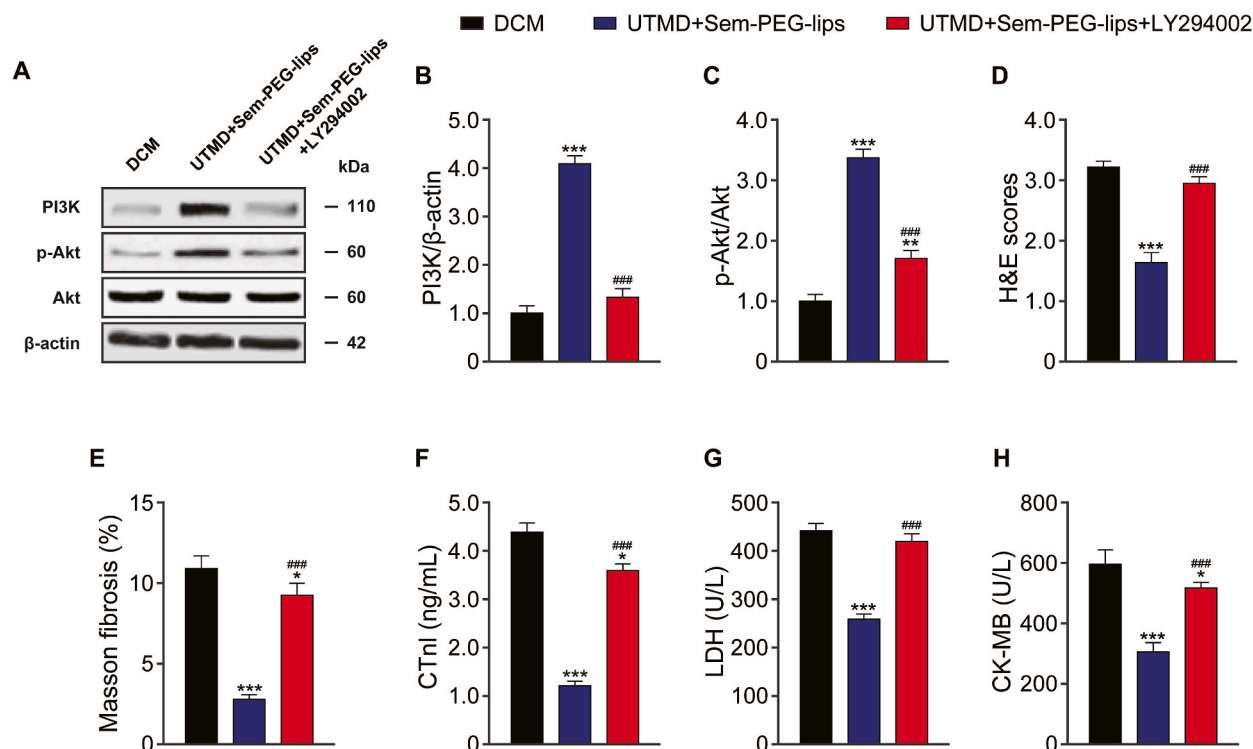


Fig. 7. Effects of UTMD combined Sem-PEG-lips on expression of PI3K/Akt/Nrf2 signaling pathway in myocardial tissue of DCM rats. (A) Representative images and expression levels of (B) PI3K and (C) *p*-Akt/Akt in myocardial tissue of DCM rats after consecutive 12 weeks intervention; (D) Representative images and expression levels of (E) Nrf2, (F) SOD2, and (G) NQO1 in myocardial tissue of DCM rats after consecutive 12 weeks intervention. Data presented as Mean ± SD, n = 5. \* $p < 0.05$ , \*\* $p < 0.01$ , \*\*\* $p < 0.001$  vs. DCM group; # $p < 0.05$ , ## $p < 0.01$ , ### $p < 0.001$  vs. UTMD + Sem-PEG-lips group.





**Fig. 8.** Inhibition of PI3K/Akt axis on beneficial effect of UTMD combined Sem-PEG-lips in DCM rats. (A) Western blot representative images and expression levels of (B) PI3K and (C) p-Akt/Akt, (D) H&E scores, (E) fibrosis% of Masson stain in myocardial tissue, and the serum levels of (F) CTnl, (G) LDH and (H) CK-MB of DCM rats after consecutive 12 weeks intervention. Data presented as Mean  $\pm$  SD,  $n = 10$ . \* $p < 0.05$ , \*\* $p < 0.01$ , \*\*\* $p < 0.001$  vs. DCM group; # $p < 0.05$ , ## $p < 0.01$ , ### $p < 0.001$  vs. UTMD + Sem-PEG-lips group.

treatment group were significantly higher than those in UTMD combined with Sem-PEG-lips group (all  $p < 0.001$ , Fig. 8F–H). The above results showed that UTMD combined with Sem-PEG-lips could improve the myocardial injury of DCM rats through PI3K/Akt axis.

#### 4. Discussion

At present, the global prevalence of diabetes mellitus is increasing year by year, and due to the poor effect of blood glucose control, it is often accompanied by different degrees of complications, which brings a huge burden to the quality of life of patients [22]. As the basic cause of diabetes, hyperglycemia can induce multiple system and organ damage, and also mediate oxidative stress and myocardial fibrosis [23]. Therefore, hyperglycemia is also an important risk factor for DCM [23]. GLP-1 is a new class of drugs for the treatment of type 2 diabetes, which can be improved by regulating the proliferation, regeneration and apoptosis of  $\beta$ -cell to enhance insulin secretion, simulate insulin action and inhibit glucagon, play a hypoglycemic effect and improve vascular endothelial dysfunction [8]. Semaglutide may have improved effects as an intestinal secreted GLP-1 analog [24]. Several clinical studies have shown that semaglutide can effectively increase the survival rate of patients after myocardial infarction and improve the cardiac function of diabetic patients [13]. Therefore, Semaglutide was used as a model drug in this study [25]. At the same time, in order to overcome the defects of poor stability, easy degradation and low bioavailability of biomacromolecule drugs *in vivo*, we applied a new water-in-water emulsification technology combined with secondary freeze-drying method, and used PEGylated phospholipids as membrane material to prepare a new type of PEGylated long circulating liposomes. Previous studies have confirmed that compared with traditional nanoliposomes, pegylated long circulating nanoliposomes loaded with drugs can prevent the drug loaded nanocarriers from being phagocytosed and degraded by the body's autoimmune system, such as phagocytes, and prolong their circulation time in the body, thus giving better play to the slow-release or controlled-release characteristics [16]. Further, the targeted release of Semaglutide at the target site was achieved by UTMD to achieve the targeted effect of the drug. Through the investigation of the properties of PEGylated circulating liposomes loaded with drugs, it was confirmed that the encapsulation efficiency of pegylated circulating liposomes prepared in this study for Semaglutide was as high as  $89.1 \pm 1.5\%$ , suggesting a good encapsulation effect of pegylated circulating liposomes.

In this study, the STZ was intraperitoneally injected into rats to establish the DM model. Compared with normal rats, the random and fasting blood glucose level of DM group rats were significantly increased, suggesting the successful construction of DM model. In addition, the body weight of DM rats was significantly lower than that of normal rats after 12 weeks. After chronic treatment, routine

echocardiography showed that the LVEF and LVFS of the DM group were significantly lower than those of the normal control group, while the levels of LVEDd, LVESD, LVEF and LVFS were significantly higher than those of the normal control group, indicating that the DM rats had obvious abnormalities of the left ventricular systolic functions at week 12. The results of histopathological observation also indicated that the myocardium of DM rats showed obvious myocardial interstitial fibrosis and cardiomyocyte apoptosis compared with the control group. These results suggest that the impairment of cardiac contractile function in DM rats may be related to myocardial interstitial fibrosis and cardiomyocyte apoptosis. Therefore, it is of great significance to effectively inhibit myocardial interstitial fibrosis and reduce cardiomyocyte apoptosis for the early prevention and treatment of DCM.

In this study, the PEG loaded nanoliposomes and SonoVue ultrasound contrast agent were mixed to make Sem-PEG-lips SonoVue microbubble suspension, which was injected into DCM rats via tail vein, and the microbubbles were exploded in the precordial region using UTMD. After 12 weeks of intervention, it was found that compared with the DCM model group, the weight of rats in the UTMD combined with Sem-PEG-lips treatment group was significantly increased, and the random blood glucose level and fasting blood glucose level were significantly decreased. The echocardiographic results showed that the LVEF and LVFS of each Sem intervention group were significantly increased, while the levels of LVEDd, LVESD, LVEF and LVFS were all significantly decreased. Compared with the other groups, the UTMD combined Sem-PEG-lips group had the most significant improvement in left ventricular systolic functions. At the same time, histopathological observation also confirmed that UTMD combined with Sem-PEG-lips had more obvious effects on inhibiting myocardial interstitial fiber degeneration and reducing cardiomyocyte apoptosis than other groups. It can be seen that ultrasound targeted destruction of Sem-PEG-lips can more significantly prevent the myocardial injuries caused by diabetes.

Myocardial hypertrophy and fibrosis are important causes of reduced cardiac function, and are also one of the main characteristics of diabetic myocardial injury [26]. This was also confirmed by the observation of myocardial pathological tissue in DCM rats. Results of Masson staining showed that the myocardial tissues of DCM rats developed fibrosis. After 12 weeks of UTMD combined with Sem-PEG-lips intervention, myocardial fibrosis in DCM rats was significantly improved and better than any other treatment, indicating that ultrasound-mediated Sem-PEG-lips can significantly inhibit diabetes-induced myocardial fibrosis. The reason may be that when Sem-PEG-lips pass through the heart blood vessels, it produces cavitation effect under ultrasonic sound energy, which promotes the release of Sem. At the same time, under the action of mechanical force, the vascular endothelial cell gap widens and the cardiomyocyte membrane forms reversible pores, making more Sem enter the cardiomyocytes to play a biological effect. However, the other forms of Sem intervention group had a weak protective effect on the heart due to the lack of ultrasound effect or the protection of pegylated nanoliposomes, and the amount of protein released into the blood circulation to exert biological effects was less. Not only that, under the shear force formed by ultrasonic micro jet, the myocardial cell membrane opens many temporary holes, so that a larger dose of Sem can enter the myocardial cell, thus exerting its biological effect of inhibiting myocardial interstitial fibrosis and reducing cardiomyocyte apoptosis, thereby improving cardiac function. Zamani et al. and won et al. found that bursting the microbubbles containing stromal cell derived factor-1 (SDF-1) under ultrasonic irradiation can increase the concentration of SDF-1 drug around the myocardial tissue [27,28]. The local release of SDF-1 from the tissue can bind with CXCR4, the only ligand on the surface of mesenchymal stem cells (MSCs), recruit MSCs to target movement, promote the proliferation and differentiation, repair the damaged myocardial tissue, and protect the myocardial tissue more effectively.

Oxidative stress is one of the important causes of pathophysiological changes in diabetes [29]. Long term exposure of organs to high glucose environment will lead to increased production of free radicals, exceeding the scavenging capacity of endogenous antioxidants, leading to MDA production and cell damage [30]. SOD, GSH PX and CAT are important antioxidant enzymes *in vivo*, and are also the main products of activated Nrf2 pathway, and play an important role in alleviating diseases related to oxidative stress [31]. Studies have found that in the fructose fed rat model of insulin resistance, allicin can activate myocardial Nrf2 through PI3K/Akt signaling pathway, and reduce oxidative stress by enhancing the antioxidant system to achieve myocardial protection [32]. Liu et al. found that syringic acid can improve myocardial ischemia-reperfusion injury by activating PI3K/Akt signaling pathway, and play a protective role on myocardium [33]. Nrf2 is an important transcription factor, which can regulate the antioxidant pathway in cells, so as to maintain cellular redox homeostasis from oxidative stress damage [34]. Activated Nrf2 can scavenge excessive reactive oxygen species [31]. Current study demonstrated that the MDA level in the cardiac tissues of DCM rats were significantly increased, while the activities of antioxidant enzymes were significantly decreased, suggesting the occurrence of oxidative stress. Similar to previous findings [32,35], the occurrence of oxidative stress in cardiac tissues of the DCM rats were accompanied by a significant decrease in the expression of PI3K and the phosphorylation level of Akt in cardiac tissues, while the expression levels of Nrf2, SOD2 and NQO1 was significantly down-regulated. In addition, different forms of Sem intervention for 12 weeks significantly reduced the level of MDA and increased the activity of related antioxidant enzymes in the myocardial tissue of DCM rats, accompanied by the increased expression of PI3K and the phosphorylation level of Akt and the up regulation of the expression of Nrf2 signaling pathway related proteins. Interestingly, the oxidative stress injury of rats in UTMD combined with Sem-PEG-lips group was significantly improved compared with other treatment groups. The above results showed that UTMD combined with Sem-PEG-lips could improve myocardial injury in diabetic rats by activating PI3K/Akt/Nrf2 signaling pathway.

In order to verify that UTMD combined with Sem-PEG-lips can improve diabetic myocardial injuries by activating PI3K/Akt axis, a rescue test were further conducted. After co-treatment of LY294002, as a PI3K inhibitor, to DCM rats, the expression level of PI3K was significantly reduced, accompanied by the reduction of Akt phosphorylation level. Interestingly, LY294002 treatment significantly aggravated the H&E score of myocardial tissue and the degree of myocardial fibrosis in DCM rats. In addition, UTMD combined with Sem-PEG-lips treatment significantly reduced the serum indicators related to myocardial injury in DCM rats. However, these changes were significantly reversed by LY294002, suggesting that inhibition of PI3K/Akt axis can significantly reduce the beneficial effect of UTMD combined with Sem-PEG-lips on diabetic myocardial injury. It is worth noting that compared with DCM rats, the phosphorylation level of Akt in UTMD + Sem-PEG-lips + LY294002 treatment group was significantly increased, and the levels of CTnl and CK-

MB in serum were significantly decreased, indicating that LY294002 treatment only partially reversed the improvement effect of UTMD combined with Sem-PEG-lips treatment, and other signaling pathways may be involved. This is a limitation of this study and deserves further attention in our follow-up study.

In conclusion, the results of current study show that ultrasound targeted destruction of Sem-PEG-lips can effectively release Semaglutide in myocardial tissue and plays role in improving STZ induced diabetic myocardial injury, protecting the left ventricular systolic function of rats. The UTMD combined with Sem-PEG-lips can effectively target and deliver the Semaglutide to myocardial tissues of DM rats, and play an anti-diabetic role in myocardial injury by activating the PI3K/Akt/Nrf2 signaling pathway, and the protective effects are better than other modalities of Semaglutide. At the same time, ultrasound targeting technology combined with long-acting PEGylated drug loaded liposomes provides a new targeted therapy for other short-term therapeutic drugs.

### Ethics statement

All the experimental procedures were performed by and approved by the Animal Experimental Ethical Inspection of the First Affiliated Hospital, Zhejiang University School of Medicine with the approval number of 2023-1005.

### Funding

This work was supported by Medical Health Science and Technology Project of Zhejiang Province (2021KY1062 and 2022KY1172).

### Author contribution statement

Jiawei Zhu: Conceived and designed the experiments; Performed the experiments; Analyzed and interpreted the data; Wrote the paper. Huiyang Wang: Performed the experiments; Analyzed and interpreted the data. Chunyang Yan; Bin Li: Performed the experiments. Bin Chen: Conceived and designed the experiments; Contributed reagents, materials, analysis tools or data. Data availability statement: Data included in article/supp. material/referenced in article. Declaration of interest's statement: The authors declare no conflict of interest.

### Declaration of competing interest

The authors have indicated no conflicts of interest.

### Acknowledgment

Not applicable.

### Appendix A. Supplementary data

Supplementary data to this article can be found online at <https://doi.org/10.1016/j.heliyon.2023.e19873>.

### References

- [1] A.L. Perdigoto, P. Preston-Hurlburt, P. Clark, S.A. Long, P.S. Linsley, K.M. Harris, S.E. Gitelman, C.J. Greenbaum, P.A. Gottlieb, W. Hagopian, A. Woodwyk, J. Dziura, K.C. Herold, Treatment of type 1 diabetes with teplizumab: clinical and immunological follow-up after 7 years from diagnosis, *Diabetologia* 62 (4) (2019) 655–664.
- [2] Z. Luo, G. Fabre, V.G. Rodwin, Meeting the challenge of diabetes in China, *Int. J. Health Pol. Manag.* 9 (2) (2020) 47–52.
- [3] I. Evangelista, R. Nuti, T. Picchioni, F. Dotta, A. Palazzuoli, Molecular dysfunction and phenotypic derangement in diabetic cardiomyopathy, *Int. J. Mol. Sci.* 20 (13) (2019) 3264.
- [4] G. Jia, V.G. DeMarco, J.R. Sowers, Insulin resistance and hyperinsulinaemia in diabetic cardiomyopathy, *Nat. Rev. Endocrinol.* 12 (3) (2016) 144–153.
- [5] H. Bugger, E.D. Abel, Molecular mechanisms of diabetic cardiomyopathy, *Diabetologia* 57 (4) (2014) 660–671.
- [6] M.M. Sung, S.M. Hamza, J.R. Dyck, Myocardial metabolism in diabetic cardiomyopathy: potential therapeutic targets, *Antioxidants Redox Signal.* 22 (17) (2015) 1606–1630.
- [7] Y. Tan, Z. Zhang, C. Zheng, K.A. Wintergerst, B.B. Keller, L. Cai, Mechanisms of diabetic cardiomyopathy and potential therapeutic strategies: preclinical and clinical evidence, *Nat. Rev. Cardiol.* 17 (9) (2020) 585–607.
- [8] L. Wu, K. Wang, W. Wang, Z. Wen, P. Wang, L. Liu, D.W. Wang, Glucagon-like peptide-1 ameliorates cardiac lipotoxicity in diabetic cardiomyopathy via the PPAR $\alpha$  pathway, *Aging Cell* 17 (4) (2018), e12763.
- [9] E. Andrikou, C. Tsioufis, I. Andrikou, I. Leontsinis, D. Tousoulis, N. Papanas, GLP-1 receptor agonists and cardiovascular outcome trials: an update, *Hellenic J. Cardiol.* 60 (6) (2019) 347–351.
- [10] K.H. Sheahan, E.A. Wahlberg, M.P. Gilbert, An overview of GLP-1 agonists and recent cardiovascular outcomes trials, *Postgrad. Med.* 96 (1133) (2020) 156–161.
- [11] J. Lau, P. Bloch, L. Schaffer, I. Pettersson, J. Spetzler, J. Kofoed, K. Madsen, L.B. Knudsen, J. McGuire, D.B. Steensgaard, The discovery of the once weekly glucagon like peptide 1 (GLP-1) analog semaglutide, *J. Med. Chem.* (2015), 150826170245001.
- [12] S.P. Marso, S.C. Bain, A. Consoli, F.G. Eliaschewitz, T. Vilsbøll, Semaglutide and cardiovascular outcomes in patients with type 2 diabetes, *N. Engl. J. Med.* 375 (19) (2016) 1834–1844.
- [13] G.B. Lim, Diabetes: cardiovascular benefits of semaglutide, *Nat. Rev. Cardiol.* 13 (12) (2016) 697.

- [14] D. Giugliano, M.I. Maiorino, G. Bellastella, M. Longo, P. Chiodini, K. Esposito, GLP-1 receptor agonists for prevention of cardiorenal outcomes in type 2 diabetes: an updated meta-analysis including the REWIND and PIONEER 6 trials, *Diabetes Obes. Metabol.* 21 (11) (2019) 2576–2580.
- [15] Y.A. Tereshkina, T.I. Torkhovskaya, E.G. Tikhonova, L.V. Kostryukova, M.A. Sanzhakov, E.I. Korotkevich, Y.Y. Khudoklinova, N.A. Orlova, E.F. Kolesanova, Nanoliposomes as drug delivery systems: safety concerns, *J. Drug Target.* 30 (3) (2022) 313–325.
- [16] A. Singh, Y.R. Neupane, B. Mangla, S. Shafi, K. Kohli, PEGylated nanoliposomes potentiated oral combination therapy for effective cancer treatment, *Curr. Drug Deliv.* 17 (9) (2020) 728–735.
- [17] S. Hernot, A.L. Klibanov, Microbubbles in ultrasound-triggered drug and gene delivery, *Adv. Drug Deliv. Rev.* 60 (10) (2008) 1153–1166.
- [18] S.T. Kang, C.K. Yeh, Ultrasound microbubble contrast agents for diagnostic and therapeutic applications: current status and future design, *Chang Gung Med. J.* 35 (2) (2012) 125–139.
- [19] Y.Z. Zhao, X. Li, C.T. Lu, M. Lin, L.J. Chen, Q. Xiang, M. Zhang, R.R. Jin, X. Jiang, X.T. Shen, X.K. Li, J. Cai, Gelatin nanostructured lipid carriers-mediated intranasal delivery of basic fibroblast growth factor enhances functional recovery in hemiparkinsonian rats, *Nanomedicine* 10 (4) (2014) 755–764.
- [20] K. Suchal, S. Malik, S.I. Khan, R.K. Malhotra, S.N. Goyal, J. Bhatia, S. Kumari, S. Ojha, D.S. Arya, Protective effect of mangiferin on myocardial ischemia-reperfusion injury in streptozotocin-induced diabetic rats: role of AGE-RAGE/MAPK pathways, *Sci. Rep.* 7 (2017), 42027.
- [21] H.X. Zheng, S.S. Qi, J. He, C.Y. Hu, H. Han, H. Jiang, X.S. Li, Cyanidin-3-glucoside from black rice ameliorates diabetic nephropathy via reducing blood glucose, suppressing oxidative stress and inflammation, and regulating transforming growth factor  $\beta$ 1/smad expression, *J. Agric. Food Chem.* 68 (15) (2020) 4399–4410.
- [22] H. Sun, P. Saeedi, S. Karuranga, M. Pinkepank, K. Ogurtsova, B.B. Duncan, C. Stein, A. Basit, J.C.N. Chan, J.C. Mbanya, M.E. Pavkov, A. Ramachandran, S. H. Wild, S. James, W.H. Herman, P. Zhang, C. Bommer, S. Kuo, E.J. Boyko, D.J. Magliano, IDF Diabetes Atlas: global, regional and country-level diabetes prevalence estimates for 2021 and projections for 2045, *Diabetes Res. Clin. Pract.* 183 (2022), 109119.
- [23] G. Jia, A. Whaley-Connell, J.R. Sowers, Diabetic cardiomyopathy: a hyperglycaemia- and insulin-resistance-induced heart disease, *Diabetologia* 61 (1) (2018) 21–28.
- [24] D. Linton, J. Blundell, G. Finlayson, M.B. Axelsen, A. Flint, C. Gibbons, T. Kvist, J. Hjerpsted, Semaglutide reduces appetite and energy intake, improves control of eating and provides weight loss in subjects with obesity, *Can. J. Diabetes* 40 (5) (2016) S3.
- [25] G. Deng, J. Ren, R. Li, M. Li, X. Jin, J. Li, J. Liu, Y. Gao, J. Zhang, X. Wang, G. Wang, Systematic investigation of the underlying mechanisms of GLP-1 receptor agonists to prevent myocardial infarction in patients with type 2 diabetes mellitus using network pharmacology, *Front. Pharmacol.* 14 (2023), 1125753.
- [26] C. Li, J. Zhang, M. Xue, X. Li, F. Han, X. Liu, L. Xu, Y. Lu, Y. Cheng, T. Li, X. Yu, B. Sun, L. Chen, SGLT2 inhibition with empagliflozin attenuates myocardial oxidative stress and fibrosis in diabetic mice heart, *Cardiovasc. Diabetol.* 18 (1) (2019) 15.
- [27] M. Zamani, M.P. Prabhakaran, E.S. Thian, S. Ramakrishna, Controlled delivery of stromal derived factor-1 $\alpha$  from poly lactic-co-glycolic acid core-shell particles to recruit mesenchymal stem cells for cardiac regeneration, *J. Colloid Interface Sci.* 451 (2015) 144–152.
- [28] Y.W. Won, A.N. Patel, D.A. Bull, Cell surface engineering to enhance mesenchymal stem cell migration toward an SDF-1 gradient, *Biomaterials* 35 (21) (2014) 5627–5635.
- [29] J.L. Rains, S.K. Jain, Oxidative stress, insulin signaling, and diabetes, *Free Radic. Biol. Med.* 50 (5) (2011) 567–575.
- [30] G. Jia, M.A. Hill, J.R. Sowers, Diabetic cardiomyopathy: an update of mechanisms contributing to this clinical entity, *Circ. Res.* 122 (4) (2018) 624–638.
- [31] I. Bellezza, I. Giambanco, A. Minelli, R. Donato, Nrf2-Keap1 signaling in oxidative and reductive stress, *Biochim. Biophys. Acta Mol. Cell Res.* 1865 (5) (2018) 721–733.
- [32] R. Padiya, D. Chowdhury, R. Borkar, R. Srinivas, M. Pal Bhadra, S.K. Banerjee, Garlic attenuates cardiac oxidative stress via activation of PI3K/AKT/Nrf2-Keap1 pathway in fructose-fed diabetic rat, *PLoS One* 9 (5) (2014), e94228.
- [33] G. Liu, B.F. Zhang, Q. Hu, X.P. Liu, J. Chen, Syringic acid mitigates myocardial ischemia reperfusion injury by activating the PI3K/Akt/GSK-3 $\beta$  signaling pathway, *Biochem. Biophys. Res. Commun.* 531 (2) (2020) 242–249.
- [34] Q. Liu, Y. Gao, X. Ci, Role of Nrf2 and its activators in respiratory diseases, *Oxid Med Cell Longev.* 2019 (2019), 7090534.
- [35] M. Zhang, N.W. Zhu, W.C. Ma, M.J. Chen, L. Zheng, Combined treatment with ultrasound-targeted microbubble destruction technique and NM-aFGF-loaded PEG-nanoliposomes protects against diabetic cardiomyopathy-induced oxidative stress by activating the AKT/GSK-3 $\beta$ 1/Nrf-2 pathway, *Drug Deliv.* 27 (1) (2020) 938–952.